IRSTI 27.35.63 https://doi.org/10.26577/ijmph.2020.v11.i1.01

**[1]B.G. Mukanova, [1]D.S. Rakisheva**

[1]L.N. Gumilyov Eurasian National University, Nur-Sultan, Kazakhstan,
e-mail: mbsha01@gmail.com, dilya784@mail.ru

# THE METHOD OF INTEGRAL EQUATIONS AND FOURIER TRANSFORMS FOR THE PROBLEMS OF MODELING THE ELECTRICAL MONITORING OF DAMS AND BARRIERS

**Abstract.** Design of electrical monitoring of dams and barriersis an actual task in geophysics. A primary purpose is an exposure of change of structure, erosion, cracks and losses of weir on the early stages. Then it is important to remove and repair a weir and prevent destructions of dike overall. For mathematical modeling of electrical monitoring of dams and barriers, the authors consider the method of ERT. The paper shows a mathematical model of the electrical survey of dams and barriers based on the method of integral equations and the Fourier transform. Numerical calculations for this model are performed. The simulation results for studying the influence of the location of the water-dam boundary with respect to the sounding array are presented. For the purposes of mathematical modeling, two extreme cases were considered: a) a fluid is assumed to be infinitely conductive, b) a fluid is not conductive, i.e. distilled. The effect of a change in the position of the supply electrode at a fixed water level was also studied. The simulation results are presented in the form of apparent resistivity curves, as it is customary in geophysical practice. Distribution of density of secondary charges is also shown for the cases of infinitely conducting and distilledwater.
**Key words:** method of integral equations, Fourier transform, apparent resistivity, electrical monitoring of dams and barriers, electrical tomography, resistivity method.

## Introduction

Mathematical modeling is currently an indispensable tool for geophysical research. In particular, modeling of electrical monitoring of dams and barriers is one of the important tasks in geophysics. Modeling the influence of changes in the dam structure, the detection of leakage zones, the appearance of erosion, changes in water levels at the upper and lower pools, dam breaks and much more associated direct and inverse problems interest many scientists [1] – [10]. In order to prevent the damage of the dam and the destruction its structure, it is necessary to identify problems of leakage and erosion in the early stages by timely monitoring. In this case, it is desirable that the measurements were carried out on the same profiles and the same grounded electrodes along seasonal and annual monitoring. One of the powerful methods for monitoring dams and barriers is the Electrical Resistivity Tomography (ERT) method. In many cases of dam monitoring, electrical tomography is performed along the dam crest and different longitudinal levels of the dam body [1] – [5]. This is due to the influence of the shape of the dam and its complex structure on the anomalies of apparent resistivities and the lack of reliable interpretation methods for profiles located across the body of the dam. However, with longitudinal soundings of the foot of the dam, where there may be leaks, and even flushing the dam, electrical tomography becomes problematic. A change in the water level at the upstream also affects the results of tomography. To solve such problems, modeling the electrical tomography of a dam across its body comes to the fore. In this paper, the authors simulate the electrical sounding of a dam across its body, using the quasi-three-dimensional model [11] based on the integral equation method [12] – [18] and the Fourier transform [11]. Studies were carried out for the following two cases: a) when the water is infinitely conductive and distilled for different water levels; b) the influence of the position of the supply electrode is studied at a constant water level. For both cases, curves of apparent resistivity are computed.

 

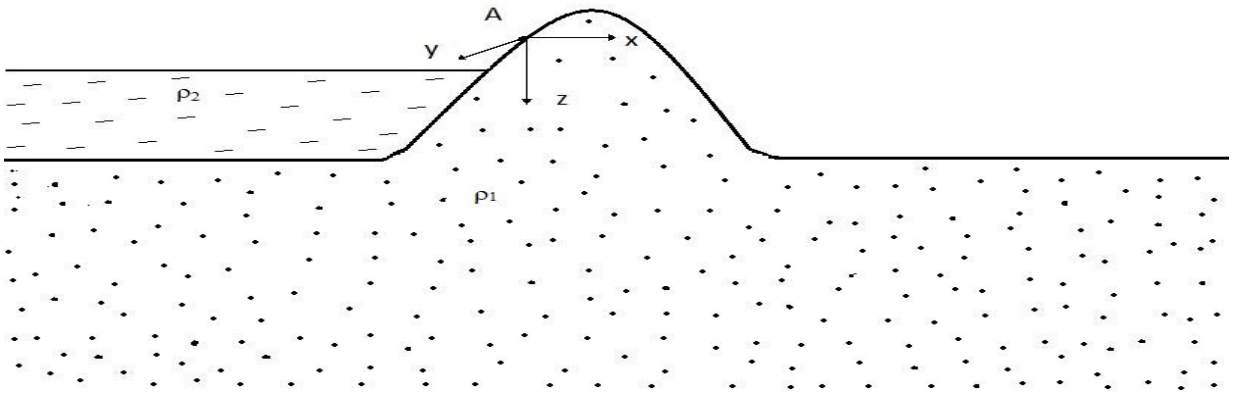


**Figure 1** – The dam model

**Mathematical model. Integral Equation and Fourier Transform**

The dam has the shape of a single shaft, to the left of which is water (Figure 1). It has been shown in the monograph [11] that for the case of homogeneous media with non-flat surface, the most adequate and computationally low-cost method is the Integral Equation Method (IEM). It has been also shown in [11] that for the case of 2D media with step-wise constant resistivity distribution, the corresponding integral equation can be reduced to series of 1D integral equations in the spectral space. After solving the problem for spectral data, the spatial distribution of the electric field is calculated using the inverse Fourier transform. The described approach significantly reduces computational costs for the 3D electric field of a point source in two-dimensional media [11].The novelty of our approach consists of application of the IEM and subsequent Fourier transform method to the media with non-flat surface, causethis case is not considered before.

Let us apply the above-mentioned methods to the considered problem. The field is excited by the direct current flowing down from the electrode $A(x_A, 0,0)$. The dam is elongated along the y axis, the direction of the normal depends only on the *x* and $z$ coordinates of the point $M(x, y, z)$. The point $P$ with coordinates $P(x', y', z')$ belong to the surface of integration. As shown in the monograph [11], the problem of electrical monitoring is reduced to a system of integral equations for the density of secondary sources (simple layer) distributed along the boundaries of contacting media. Let $q_0(x,y,z)$ and $q_{12}(x,y,z)$ be the densities of a simple layer of secondary charges distributed along the dam-air surface and along the water-dam boundary. Under the assumption that the electrical conductivity of water is much greater than the conductivity of the dam body, and literally applyingthe method of the monograph [11], we write the following integral equations:

$$q_0(x,y,z) = -\frac{1}{2\pi}\iint_{\Gamma^0} q_0(x',y',z')\frac{\partial}{\partial n_M^0} G\left(\frac{1}{(xx',yy',zz')}\right) d\Gamma_p^0 + \frac{\partial}{\partial n^0} G\left(\frac{1}{2\pi(xx_A,yy_A,zz_A)}\right) \quad (1)$$

$$q_{12}(x,y,z) = -æ_{12}\frac{1}{2\pi}\iint_{\Gamma^{12}} q_{12}(x',y',z')\frac{\partial}{\partial n_M^{12}} G\frac{d\Gamma^{12}}{(xx',yy',zz')} -$$

$$æ_{12}\frac{1}{2\pi}\iint_{\Gamma^0} q_0(x',y',z')\frac{\partial}{\partial n_M^{12}} G\frac{\partial\Gamma^0}{(xx',yy',zz')} + æ_{12}\frac{\partial}{\partial n^{12}} G\left(\frac{1}{2\pi(xx_A,yy_A,zz_A)}\right) \quad (2)$$

Here $G(x,x',y,y',z,z')$ is is the Green's function of the problem, which depends on the following arguments $G(x,x',y-y',z,z')$. In formulas (1), (2), the functions are differentiated along the direction of the external normal to the boundary at the point $M(x,y,z)$.

Note that integration over the surfaces $\Gamma^0$ и $\Gamma^{12}$ can be represented as a sequential integration over a generator directed along the y axis, and then along the contours $L_0$ and $L_{12}$ respectively. $L_0$is the contour of the surface $\Gamma^0$, and $L_{12}$ s the contour of $\Gamma^{12}$. Since the dam is elongated along the y axis, formulas (1), (2) can be written in the following form:

$$q_0(x,y,z) = \frac{\partial}{\partial n^0} G\left(\frac{1}{2\pi(xx_A, y-y_A, zz_A)}\right) - \frac{1}{2\pi}\int_{L_0} \int_{-\infty}^{+\infty} q_0(x',y',z') \frac{\partial}{\partial n_M^0} G\left(\frac{1}{(xx', y-y', zz')}\right) dy' dL_0 \quad (3)$$

$$q_{12}(x,y,z) = \frac{æ_{12}}{2\pi}\frac{\partial}{\partial n^{12}} G\left(\frac{1}{(xx_A, y-y_A, zz_A)}\right) - æ_{12}\frac{1}{2\pi}\iint_{L_T-\infty}^{+\infty} q_{12}(x',y',z') \frac{\partial}{\partial n_M^{12}} G \frac{dy' dL_T}{(xx', y-y', zz')} + æ_{12}\frac{1}{2\pi}\iint_{L_1-\infty}^{+\infty} q_0(x',y',z') \frac{\partial}{\partial n_M^0} G\left(\frac{1}{(xx_A, y-y_A, zz_A)}\right) dy' dL_s \quad (4)$$

The internal integrals in equations (3), (4) are the convolution integrals of the function $q_0(x',y',z')$ and $\frac{\partial}{\partial n_M^0} G\left(\frac{1}{(xx',y-y',zz')}\right)$with respect to the coordinate y. The coefficient $æ_{12}$ depends on the resistivities of the dam and the water, and is equal to +1 or -1 for a conductive and non-conductive fluid, respectively.

Next, we move to the spectral space. Since the functions $q_0(x,y,z)$, $q_0(x',y',z')$, $\frac{\partial}{\partial n_M^0} G\left(\frac{1}{(xx',y-y',zz')}\right)$ and $\frac{\partial}{\partial n^0} G\left(\frac{1}{(xx_A,y-y_A,zz_A)}\right)$ are even functions with respect to the variable y, we use the partial cosine Fourier transform [11]:

$$\tilde{q}_0(x,k_y,z) = 2\int_0^{\infty} q_0(x,y,z)\, cos\, cos(k_y \cdot y) dy$$

$$\tilde{q}_0(x',k_y,z') = 2\int_0^{\infty} q_0(x',y',z')\, cos\, cos(k_y \cdot y) dy$$

$$\frac{\tilde{\partial}}{\partial n_M^0} G\left(\frac{1}{(xx',k_y,zz')}\right) = 2\int_0^{\infty} \frac{\partial}{\partial n_M^0} G\left(\frac{1}{(xx',y-y',zz')}\right) cos\, cos(k_y \cdot y) dy$$

$$\frac{\tilde{\partial}}{\partial n^0} G\left(\frac{1}{(xx_A,k_y,zz_A)}\right) = 2\int_0^{\infty} \frac{\partial}{\partial n^0} G\left(\frac{1}{(xx_A,y-y_A,zz_A)}\right) cos\, cos(k_y \cdot y) dy$$

By virtue of the two-dimensional geometry of the medium, the normal **n** does not depend on the coordinate *y*; therefore, the Fourier transform and differentiation commute.

Spectra $\tilde{q}_0(x,k_y,z)$, $\tilde{q}_0(x',k_y,z')$, $\frac{\widetilde{\partial}}{\partial n_M^0} G\left(\frac{1}{(xx',k_y,zz')}\right)$ and $\frac{\widetilde{\partial}}{\partial n^0} G\left(\frac{1}{(xx_A,y-y_A,zz_A)}\right)$ are the amplitudes of spatial harmonics with respect to frequency. Then the integral equation (3) after the cosine Fourier transform takes the form:

$$\tilde{q}_0(x,k_y,z)=\frac{1}{2\pi}\frac{\partial}{\partial n^0}G\left(\frac{1}{(xx_A,k_y,zz_A)}\right)-$$
$$\frac{1}{2\pi}\iint\limits_{L_s}^{\infty}\left[\int_{-\infty}^{+\infty}q_0(x',y',z')\frac{\partial}{\partial n_M^0}G\left(\frac{1}{(xx',y-y',zz')}\right)dy'\right]\cdot cos\ cos(k_y\cdot y')dy'dL_0 \quad (5)$$

$\int_0^{+\infty}\int_{-\infty}^{+\infty}q_0(x',y',z')\frac{\partial}{\partial n_M^0}G\left(\frac{1}{(xx',y-y',zz')}\right)$ of the functions under convolution. Hence, $cos\ cos(k_y y)dy'dy$ – is the product of the spectra

$$\tilde{q}_0(x,k_y,z)=\frac{1}{2\pi}\frac{\partial}{\partial n^0}G\left(\frac{1}{(xx_A,y-y_A,zz_A)}\right)-\frac{1}{2\pi}\int_{L_0}\tilde{q}_0(x',k_y,z')\widetilde{\frac{\partial}{\partial n_M^0}}G\left(\frac{1}{(xx',k_y,zz')}\right)dL_0 \quad (6)$$

We perform the same procedure for the integral equation (4):

$$\tilde{q}_{12}(x,k_y,z)=2\int_0^{\infty}q_0(x,y,z)\ cos\ cos(k_y\cdot y)dy$$

$$\tilde{q}_{12}(x,k_y,z)=2\int_0^{\infty}q_{12}(x',y',z')\ cos\ cos(k_y\cdot y)dy$$

$$\frac{\tilde{\partial}}{\partial n_M^{12}}G\left(\frac{1}{(xx',k_y,zz')}\right)=2\int_0^{\infty}\frac{\partial}{\partial n_M^{12}}G\left(\frac{1}{(xx',y-y',zz')}\right)cos\ cos(k_y\cdot y)dy$$

$$\frac{\tilde{\partial}}{\partial n^{12}}G\left(\frac{1}{(xx_A,k_y,zz_A)}\right)=2\int_0^{\infty}\frac{\partial}{\partial n^{12}}G\left(\frac{1}{(xx_A,y-y',zz_A)}\right)cos\ cos(k_y\cdot y)dy$$

So, the equation (4) takes the form:

$$\tilde{q}_{12}(x,k_y,z)=\frac{æ_{12}}{2\pi}\frac{\tilde{\partial}}{\partial n^{12}}G\left(\frac{1}{xx_A,k_y,zz_A}\right)-\frac{æ_{12}}{2\pi}\int_{L_{12}}\tilde{q}_{12}(x',k_y,z')\frac{\tilde{\partial}}{\partial n_M^{12}}G\left(\frac{1}{xx',k_y,zz'}\right)dL_{12}+$$
$$+\frac{æ_{12}}{2\pi}\int_{L_0}\tilde{q}_0(x',y',z')\frac{\tilde{\partial}}{\partial n_M^{12}}G\left(\frac{1}{xx',k_y,zz'}\right)dL_0 \quad (7)$$

Integral equations (6), (7) is the cosine Fourier transform of the system of integral equations (1), (2).

For a homogeneous half-space the expression in the integral equation (6) is written as:

$$\frac{\partial}{\partial n_M^0}G(x,x',y-y',z,z')=\frac{\rho}{\pi r^3}\mathbf{rn}$$

$$\frac{\partial}{\partial n_M^0}G(x,x_A,y-y_A,z,z_A)=\frac{\rho}{\pi r^3}\mathbf{rn}$$

where **n** is the unit vector of the external normal to the surface $\Gamma^0$ at the point (*x, y, z*). Given by (**1**y · *n*) = 0, for the spectra $\frac{\tilde{\partial}}{\partial n_M^0}G(x,x',k_y,z,z')$and $\frac{\tilde{\partial}}{\partial n_M^0}G(x,x_A,k_y,z,z_A)$ we obtain the following expressions:

$$\frac{\tilde{\partial}}{\partial n_M^0} G\left(\frac{1}{xx', k_y, zz'}\right) = \frac{1}{2\pi}[(x-x')\cdot(n_x) + (z-z')(n_z)] \int_0^\infty \frac{cos\ cos(k_y \cdot y)}{(R^2+y^2)^{\frac{3}{2}}} dy \quad (8)$$

$$\frac{\tilde{\partial}}{\partial n^0} G\left(\frac{1}{xx_A, k_y, zz_A}\right) = \frac{1}{2\pi}[(x-x_A)(n_x) + (z)(n_z)] \int_0^\infty \frac{cos\ cos(k_y \cdot y)}{(R_A^2+y^2)^{3/2}} dy \quad (9)$$

Here $R^2 = (x-x')^2 + (z-z')^2$, $R_A^2 = (x-x_A)^2 + (z-z_A)^2$. The values of the $R$,$R_A$ represent projections of the distances $r$, $r_A$onto the plane *xOz* respectively.

For the second integral equation, we have similarly:

$$\frac{\partial}{\partial n_M^{12}} G(x, x', y-y', z, z') = \frac{\rho}{\pi r^3}\mathbf{rn}$$

$$\frac{\partial}{\partial n_M^{12}} G(x, x_A, y-y_A, z, z_A) = \frac{\rho}{\pi r^3}\mathbf{rn}$$

where $\mathbf{n} = (n_x, n_y, n_z)$ – is the unit vector of the external normal to the surface $\Gamma^{12}$ also at the point $M(x,y,z)$. Take into account that (**1y** · **n**) = 0:

$$\frac{\tilde{\partial}}{\partial n_M^{12}} G\left(\frac{1}{(xx', k_y, zz')}\right) = \frac{æ_{12}}{2\pi}[(x-x')\cdot(n_x) + (z-z')\cdot(n_z)] \int_0^\infty \frac{cos\ cos(k_y \cdot y')}{(R^2+y'^2)^{\frac{3}{2}}} dy' \quad (10)$$

$$\frac{\tilde{\partial}}{\partial n^{12}} G\left(\frac{1}{(xx_A, k_y,\ zz_A)}\right) = \frac{æ_{12}}{2\pi}[(x-x_A)\cdot(n_x) + (z-z_A)(n_z)] \int_0^\infty \frac{cos\ cos(k_y \cdot y')}{(R^2+y'^2)^{\frac{3}{2}}} dy' \quad (11)$$

In formulas (8)-(10) there is a cosine transformation of the functions of the form $\frac{I}{(a^2+y^2)^{\frac{3}{2}}}$ where $a = const$. For this transformation we have:

$$S(k_y, a) =$$

$$\int_0^\infty \frac{cos\ cos(k_y \cdot y)}{(a^2+y^2)^{\frac{3}{2}}} dy = \frac{k_y}{2a} K_1(a \cdot k_y)$$

where $K_1(x)$ – is the MacDonald function (modified Bessel function of the second kind) of the first order. In numerical solutions of integral equations (6), (7), standard libraries of Fortran for the function $K_1(x)$ are used to compute $\frac{\partial}{\partial n_M^0} G\left(\frac{1}{|PM|}\right)$ and $\frac{\partial}{\partial n_M^0} G\left(\frac{1}{|AM|}\right)$. In order to reduce (6), (7) to the system of linear algebraic equation (SLAE), the contours $L_0$ and $L_{12}$ are divided into elements $\Delta l_0$ и $\Delta l_{12}$ within which $q_0(x,y,z)$, $q_{12}(x',y',z')$ are considered constant. Having found the spectral density of secondary sources $q_0$, we pass to spatial variables using the inverse Fourier cosine transform:

$$q_0(x,y,z) = \frac{1}{\pi}\int_0^\infty \tilde{q}_0(x, k_y, z)\cos(k_y \cdot y) dk_y \quad (12)$$

Next, based on the computed density of the secondary charges, we calculate the electric field potential by integration over the corresponding surface.

**Numerical implementation.**

The numerical solution of the integral equations was carried out by discretizing formulas (6), (7) and (12) on a logarithmic grid with respect to frequency. To calculate the cosine – Fourier transform, we consider the finite part of the boundaries $\Gamma_0$ and $\Gamma_{12}$. Uniform grids are built at the boundaries of dam-air and dam-water. The shape of the boundaries are approximated by the radial basis function (RBF)

method [19] – [22]. At the dam-air interface, we take into account that no current flows into the air; and at the water-dam boundary, the current flows down depending on the resistivity of the media. The supply electrode is located on the dam. In the calculations, the height of the water and the position of the supply electrode are varied. The field potential is computed at points corresponding to the location of the measuring electrodes. Then, through the potential differences of the field, the apparent resistivity of the medium are calculated by standard formulas.

Numerical solutions are made for the following cases:

1. The position of the water-dam boundary was changed when the water was supposed to be infinitely conductive and distilled. However, even the second case is quite rare in practice, it is interesting from the point of view of mathematical modeling. This will determine the nature of the anomalies of apparent resistivity if the resistivity of the dam material is significantly less than the resistivity of the liquid. Based on the calculated electric field, apparent resistivity curves are constructed.

2. The position of the source electrode is changed when the water level stays the same, and curves of apparent resistivity are also plotted.

Figures 2 a) and b) show the density distribution of a simple layer q (M) at the air-dam boundary $\Gamma^0$ when the water is infinitely conductive, the value is $æ_{12}$= +1 and when the water is distilled, with the value is $æ_{12}$= -1, respectively.

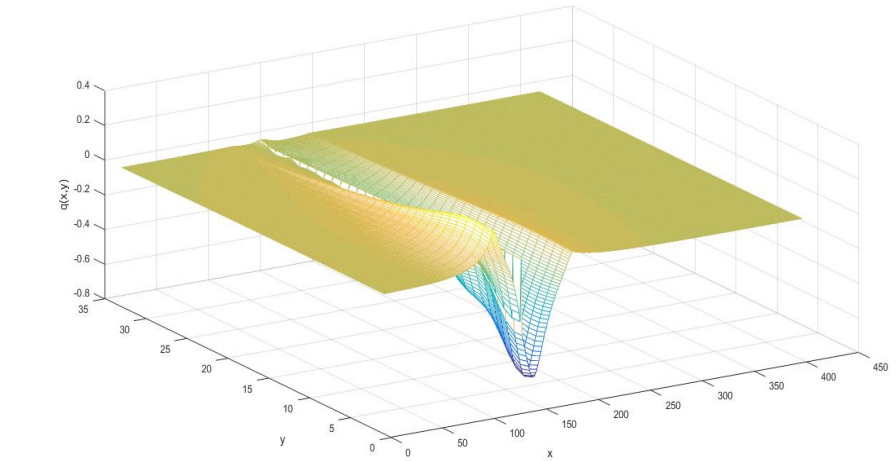


a)

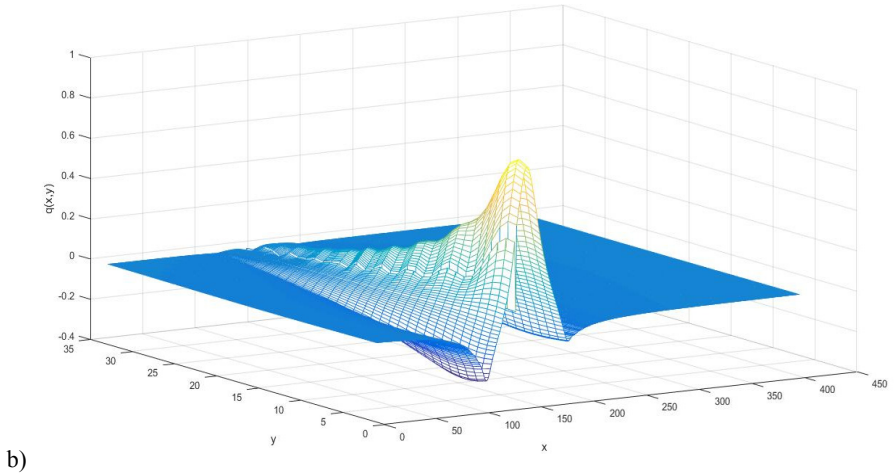


b)

**Figure 2 –** The density distribution of a simple layer q (M) on the surface $\Gamma^0$, achieved using the Fourier transform method, when water is infinitely conductive(a), and for distilled water (b)

Figure 2 shows the distribution of the simple layer density q (M) on the surface $\Gamma^0$ obtained after the Fourier transform when the water is infinitely conductive (a), and when the water is distilled (b). In Figure 3 corresponding apparent resistivity curves are demonstrated also.

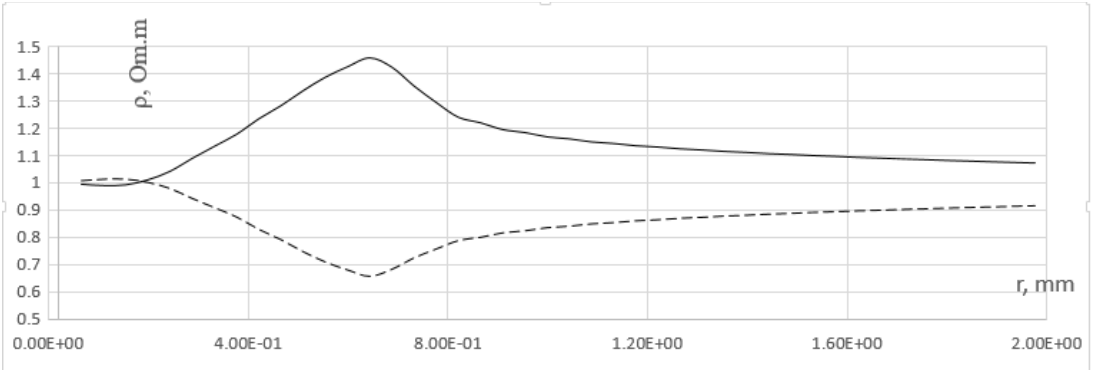


**Figure 3 –** Apparent resistivity curves
(-) – distilled water, (-) – infinitely conductive water

This test shows that for infinitely conductive water, the apparent resistivity curve is inverted with respect to the second case, as the current flows into the water.

The second test was conducted under conditions when the dam resistivity is $\rho_1$=10, and the water resistivity is $\rho_2$=100. The position of the supply electrode is changed: it was assumed that Apos = 16m, 18m, 20m from the origin, the water level does not change and is placed at the point at a distance of Cpos = 10m from the origin (Figure 4).

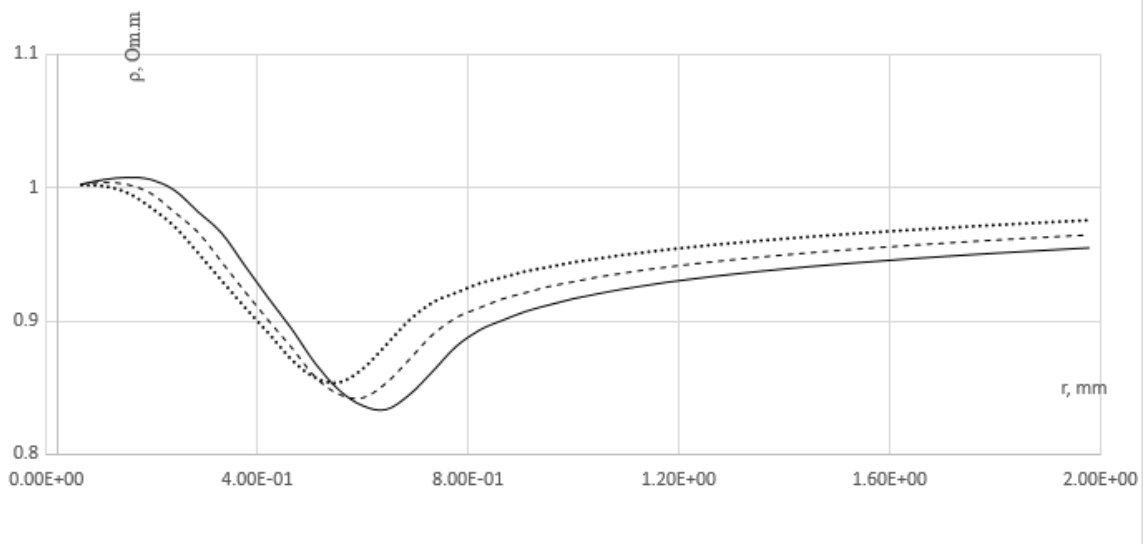


**Figure 4 –** Curves of apparent resistivity at the position of the source electrode
(-) Apos = 16m, (--) Apos = 18m, (…) Apos = 20m

Figure 4 illustrates the apparent resistivity curves at the positions of the source electrode Apos = 16m, Apos = 18m and Apos = 20m. It can be seen that the proximity of the liquid to the source electrode increases the amplitude of the anomaly in the apparent resistivity of the medium.

**Conclusion**

In a numerical solution, there is an investigation of the behavior of the apparent resistivity curves for infinitely conductive and distilled water. It is shown that in these cases the anomalies are of the opposite nature. These curves are in agreement with geophysical studies. It is also shown how the position of the source electrode affects the apparent resistivity curves at a constant water level.

Authors express their deep gratitude to the anonymous reviewer whose comments helped improve the presentation of the results.

**References**

1. Sjödahl P., Dahlin T., Johansson S., Loke M.H. «Resistivity monitoring for leakage and internal erosion detection at Hällby embankment dam», Journal of Applied Geophysics 65,2008, 155–164

2. Sjödahl P., Dahlin T., Johansson S. «Embankment dam seepage evaluation from resistivity monitoring data», Near Surface Geophysics, 2009, 463-474

3. Chih-Ping Lin, Yin-Chun Hung, Po-Lin Wu, Zen-Hung Yu «Performance of 2-D ERT in Investigation of Abnormal Seepage: A Case Study at the Hsin-Shan Earth Dam in Taiwan», Journal of Environmental and Engineering Geophysics 2017, p:101-112

4. In-Ky Cho, Ik-Soo Ha , Ki-Seog Kim , Hee-Yoon Ahn , Seunghee Lee, Hye-Jin Kang «3D effects on 2D resistivity monitoring in earth-fill dams», Near Surface Geophysics, 2014, 12, 73-81

5. Bolève A., Revil A., Janod F., Mattiuzzo J.L. and Fry J.-J. «Preferential fluid flow pathways in embankment dams imaged by self-potential tomography», Near Surface Geophysics, 2009, 447-462

6. Zerkal Evgeny «Interpretation of electrical resistivity tomography monitoring data of the Boguchan hydroelectric power plant rockfill dam», Proceedings of the 12th SEGJ International Symposium, 2015, 20-24

7. Shevnin V.A., Bobachev A.A., Ivanova S.V., «Rezultaty primeneniia metodov estestvennogo polia i elektrotomografii dlia izucheniia Aleksandrovskogo gorodishcha (Kaluzhskaia oblast)[The results of applying the methods of the natural field and electrotomography to study the Alexander settlement (Kaluga region)]», Notes of the Mining Institute. T.211 Petersburg 201, 35-42

8. Bolshakov D.K., Kozlov O.V., Modin I.N. «Vozmozhnosti elektrotomografii dlia monitoringa filtratsionnykh protsessov v tele kamenno-nabrosnoi plotiny vo vremia napolneniia vodokhranilishcha [Possibilities of electrotomography for monitoring filtration processes in the body of a rock-fill dam during reservoir filling]». VIII International Scientific and Practical Conference and Exhibition, " Engineering Geophysics - 2012", Moscow, Russia, 2012, 83-93

9. Pavlova A.M. «Primenenie maloglubinnoi elektrorazvedki dlia izucheniia trekhmerno neodnorodnykh sred [The use of shallow electrical exploration for the study of three-dimensionally inhomogeneous media]», The dissertation for the degree of candidate of technical sciences. Moscow – 2014

10. Kozlov O.V., Pavlova A.M. «Geoelektricheskii monitoring kamenno-nabrosnoi plotiny Boguchanskoi GES metodom elektrotomografii [Geoelectric monitoring of the rock-fill dam of the Boguchanskaya hydroelectric station]». Engineering survey, 12/2013, P. 40-47.

11. Mukanova B., Modin I., The Boundary Element Method in Geophysical Survey, Springer, t: 4, 2017

12. Balgaisha Mukanova, Tolkyn Mirgalikyzy and Dilyara Rakisheva, «Modelling the Influence of Ground Surface Relief on Electric Sounding Curves Using the Integral Equations Method», Mathematical Problems in Engineering.-Volume 2017, 210-215

13. Balgaisha Mukanova, A numerical solution to the well resistivity-sounding problem in the axisymmetric case, Invers problems in science and engineering-Volume -21-5 Published -2012., 767-780

14. Mukanova B., Mirgalikyzy T. Modeling the impact of relief boundaries in solving the direct problem of direct current electrical sounding Communications in Computer and Information Science, Mathematical Modeling of Technological Processes: International Conference, CITech-2015. – Almaty: Proceedings, Springer, 2015. 117-123.

15. Mirgalikyzy T., Mukanova B., Modin I. Method of Integral Equations for the Problem of Electrical Tomography in a Medium with Ground Surface Relief, Journal of Applied Mathematics. – 2015

16. Mukanova B., Mirgalikyzy T. (2015) Modeling the Impact of Relief Boundaries in

Solving the Direct Problem of Direct Current Electrical Sounding. In: Danaev N., Shokin Y., Darkhan AZ. (eds) Mathematical Modeling of Technological Processes. Communications in Computer and Information Science, vol 549. Springer, Cham.

17. Mukanova B.G., Mirkaliqizi T, Rakisheva D.S., «Modelirovanie vliianiia relefa zemnoi poverkhnosti na krivye elektricheskogo zondirovaniia metodom integralnykh uravnenii [Modeling the effect of the earth's relief on electric sounding curves by the method of integral equations]», II International Scientific Conference «Informatics and Applied Mathematics» II. – Almaty, 2017. – P.352-366.

18. B. Mukanova, T. Mirgalikyzy, M. Turarova, Numerical aspects of the adaptive computational grid in solving the problems of electrical prospecting with direct current, International Journal of Mathematics and Physics 9, No2, 4 (2018), 4-12

19. Grady B. Wright Radial Basis Function Interpolation: Numerical and Analytical Developments, Doctoral Dissertation. - Colorado, 2003, 155

20. Nail A. Gumerov, Ramani Duraiswami Fast Radial Basis Function interpolation via preconditioned Krylov Iteration. - URL: http:// www.umiacs.umd.edu/ ~ramani/ pubs/ Gumerov Duraiswami IterativeRBF06.pdf

21. Xin Yin, Weiwei Xu, Ryo Akama and Hiromi T.Tanaka A Synthesis of 3-D Kabuki Face from Ancient 2-D Images Using Multilevel Radial Basis Function. - URL: http:// www.art-science.org/ journal/ v7n1/ v7n1pp14/ artsci-v7n1pp14.pdf

22. Rakisheva D.S., Mirgalikyzy T., Mukanova B.G., «Approksimatsiia poverkhnosti relefa dnevnoi poverkhnosti metodom RBF [Approximation of the surface relief of the surface by the RBF method]», Bulletin of the National Academy of Sciences of the Republic of Kazakhstan. V. 1, N. 365, Published 2017, 210-215